

B Baryon Production and Decays and B Hadron Lifetimes

S. Donati* †

University and INFN Pisa, Largo B. Pontecorvo, 3 - 56127 Pisa, Italy

E-mail: simone.donati@pi.infn.it

In this paper we review the most recent results concerning B Baryons at CDF and D0, including the observation and the study of the properties of the Ω_b^- , Ξ_b^- and $\Sigma_b^{\pm(*)}$, the observation of new Λ_b^0 decay modes, and a new measurement of the lifetime of the b hadrons in decays with a J/ψ . The Ω_b^- baryon is observed through the decay chain $\Omega_b^- \rightarrow J/\psi \Omega^-$, where $J/\psi \rightarrow \mu^+ \mu^-$, $\Omega^- \rightarrow \Lambda K^-$, and $\Lambda \rightarrow p K^-$, using 4.2 fb^{-1} of data. The Ω_b^- mass is measured to be $6054.4 \pm 6.8(\text{stat.}) \pm 0.9(\text{syst.}) \text{ MeV}/c^2$, and the lifetime $1.13_{-0.40}^{+0.53}(\text{stat.}) \pm 0.02(\text{syst.}) \text{ ps}$. For the Ξ_b^- the mass is measured $5790.9 \pm 2.6(\text{stat.}) \pm 0.8(\text{syst.}) \text{ MeV}/c^2$ and the lifetime $1.56_{-0.25}^{+0.27}(\text{stat.}) \pm 0.02(\text{syst.}) \text{ ps}$.

A new accurate measurement of the properties of the resonances Σ_b^+ , Σ_b^- , Σ_b^{*+} , and Σ_b^{*-} has been performed in 6 fb^{-1} of data, and the masses have been determined, $m(\Sigma_b^+) = 5811.2_{-0.8}^{+0.9}(\text{stat.}) \pm 1.7(\text{syst.})$, $m(\Sigma_b^-) = 5815.5_{-0.5}^{+0.6}(\text{stat.}) \pm 1.7(\text{syst.})$, $m(\Sigma_b^{*+}) = 5832.0 \pm 0.7(\text{stat.}) \pm 1.8(\text{syst.})$, and $m(\Sigma_b^{*-}) = 5835.0 \pm 0.6(\text{stat.}) \pm 1.8(\text{syst.})$.

The $\Lambda_b^0 \rightarrow \Lambda_c^+ \pi^- \pi^+ \pi^-$ decay mode has been observed in 2.4 fb^{-1} of data, with the resonant decay modes $\Lambda_b^0 \rightarrow \Lambda_c(2595)^+ \pi^- \rightarrow \Lambda_c^+ \pi^- \pi^+ \pi^-$, $\Lambda_b^0 \rightarrow \Lambda_c(2625)^+ \pi^- \rightarrow \Lambda_c^+ \pi^- \pi^+ \pi^-$, $\Lambda_b^0 \rightarrow \Sigma_c(2455)^{++} \pi^- \pi^- \rightarrow \Lambda_c^+ \pi^- \pi^+ \pi^-$, and $\Lambda_b^0 \rightarrow \Sigma_c(2455)^0 \pi^+ \pi^- \rightarrow \Lambda_c^+ \pi^- \pi^+ \pi^-$.

CDF has performed new measurements of the b hadron lifetimes in decays with a J/ψ . The measured lifetimes are the currently most precise determination of the B^+ , B^0 and Λ_b^0 lifetimes. The measured values are $c\tau(B^+) = 491.4 \pm 2.6(\text{stat.}) \pm 2.6(\text{syst.}) \mu\text{m}$, $c\tau(B^0) = 451.7 \pm 3.0(\text{stat.}) \pm 2.5(\text{syst.}) \mu\text{m}$, and $c\tau(\Lambda_b^0) = 460.8 \pm 13.4(\text{stat.}) \pm 4.1(\text{syst.}) \mu\text{m}$.

FPCP 2010 - 8th Flavour Physics and CP Violation 2010

May 25 - 29, 2010

Torino, Italy

*Speaker.

† for the CDF and D0 Collaborations

1. Introduction

B hadrons are abundantly produced at the Tevatron Collider, where the measured b production cross section is $\sigma(B^+) = 2.78 \pm 0.24 \mu\text{b}$ for $p_T(B^+) \geq 6 \text{ GeV}/c$ and $|y| \leq 1$ ([1]), and the available energy allows the production of the heavier Λ_b , Σ_b , Ξ_b and Ω_b hadrons. The challenge is extracting signals from background which are orders of magnitude higher at production. This is achieved with dedicated detectors and triggers.

The CDF II tracker is made of three silicon detectors ([3]) and a drift chamber ([4]) located within a solenoidal magnetic field. Particle identification is performed with the measurement of the specific ionisation in the drift chamber and of the time of flight in a specific detector ([5]). Segmented electromagnetic and hadronic calorimeters surround the tracking system ([6]). The muon detectors ([7]) are located outside the central hadron calorimeter. CDF II uses a three-level trigger system. The heart of the L1 trigger is the eXtremely Fast Tracker ([8]), the trigger track processor that identifies charged tracks in the drift chamber. The L1 tracks are extrapolated to the calorimeter and to the muon chambers to generate electron and muon trigger candidates. The Online Silicon Vertex Tracker ([9]) is part of the L2 trigger. It receives the L1 tracks and the digitised pulse heights on the axial layers of the silicon vertex detector. It links the L1 tracks to the silicon hits and reconstructs tracks with offline-like quality, used to select online the secondary vertices characteristic of the b events in specific triggers. L3 trigger uses a CPU farm which allows to perform an almost offline-quality reconstruction.

The D0 detector [10] uses an excellent central tracking system which consists of a silicon microstrip tracker and a central fiber tracker surrounded by a solenoidal magnet and provides signals to the Level 2 and Level 3 trigger systems to select events with displaced vertices from b -quark decay. The D0 calorimeter system consists of three sampling calorimeters (primarily uranium/liquid-argon) and an intercryostat detector. The muon system uses proportional drift tubes, mini drift tubes, and toroidal magnets and provides a coverage to $|\eta| \approx 2.0$.

2. Observation and properties of the Ω_b^- and Ξ_b^- baryons

The Ω_b^- observation is made at D0[12] and CDF[11] through the decay chain $\Omega_b^- \rightarrow J/\psi \Omega^-$, where $J/\psi \rightarrow \mu^+ \mu^-$, $\Omega^- \rightarrow \Lambda K^-$, and $\Lambda \rightarrow p \pi^-$. The Ξ_b^- is reconstructed through the similar decay mode $\Xi_b^- \rightarrow J/\psi \Xi^-$, where $J/\psi \rightarrow \mu^+ \mu^-$, $\Xi^- \rightarrow \Lambda \pi^-$, and $\Lambda \rightarrow p \pi^-$ as a crosscheck. The CDF analysis selects well-measured $J/\psi \rightarrow \mu^+ \mu^-$ candidates, where the two-muon invariant mass is required within $80 \text{ MeV}/c^2$ of the world-average J/ψ mass. Λ candidates use all opposite charge track pairs with $p_T > 0.4 \text{ GeV}/c$ found in the chamber. The proton (pion) mass is assigned to the track with the higher (lower) momentum, which is correct for the Λ candidates used in this analysis for the kinematics of the Λ decay and the lower limit in the transverse momentum acceptance of the tracking system. The additional tracks are assigned the pion or kaon mass, and $\Lambda \pi^-$ and ΛK^- combinations are identified that are consistent with the decay process $\Xi^- \rightarrow \Lambda \pi^-$ or $\Omega^- \rightarrow \Lambda K^-$. The charged hyperon candidates have an additional fit performed with the three tracks that simultaneously constrains the Λ and Ξ^- or Ω^- masses of the appropriate track combinations and provides the best possible estimate of the hyperon momentum and decay position. A significant background reduction is achieved by requiring the charged hyperon candidates have track measurements in at

least one layer of the silicon detector. The shorter lifetime of the Ω^- makes the silicon selection not efficient in compare to the Ξ^- . For this reason silicon detector information on the hyperon track is used when it is available, but it is not imposed as a requirement for the Ω^- selection. The hyperon candidates are combined with the J/ψ candidates by fitting the five-track state with constraints appropriate for each decay topology and intermediate hadron state. The $\mu^+\mu^-$ mass is constrained to the nominal J/ψ mass, and the hyperon candidate is constrained to originate from the J/ψ decay vertex. The fits that include the charged hyperon constrain the Λ candidate tracks to the nominal Λ mass, and the Ξ^- and Ω^- candidates to the respective nominal masses. b -hadron candidates are required to have $p_T > 6.0$ GeV/c and the hyperon to have $p_T > 2.0$ GeV/c. Figure 1 shows the CDF Ξ_b^- and Ω_b^- mass distributions.

CDF measures a Ξ_b^- mass to be $5790.9 \pm 2.6(\text{stat.}) \pm 0.8(\text{syst.})$ MeV/c² and the Ω_b^- to be $6054.4 \pm 6.8(\text{stat.}) \pm 0.9(\text{syst.})$ MeV/c². The systematic errors are due to the uncertainty on the mass scale of the baryons measured with the hyperons in the final state, estimated as the mass difference between the B^0 as measured in the $J/\psi K_s^0$ and the nominal B^0 mass and rescaled for the different energy measured by the tracking system in the two decay modes. A systematic error is due to the dependence of the measured on the alternative assumption to have a constant or an event-by-event mass resolution in the fit. A further systematic is due to the uncertainty on the Ω^- mass. The Ξ_b^- lifetime is measured to be $1.56_{-0.25}^{+0.27}(\text{stat.}) \pm 0.02(\text{syst.})$ ps and the lifetime of the Ω_b^- to be $1.13_{-0.40}^{+0.53}(\text{stat.}) \pm 0.02(\text{syst.})$ ps. The systematic errors are due to the treatment of the resolution on the proper decay length in the fit ($2 \mu\text{m}$), to the detector mis-alignment ($1 \mu\text{m}$). The productions of the Ξ_b^- and of the Ω_b^- relative to the Λ_b^0 are found to be $\frac{\sigma(\Xi_b^-)BR(\Xi_b^- \rightarrow J/\psi \Xi^-)}{\sigma(\Lambda_b^0)BR(\Lambda_b^0 \rightarrow J/\psi \Lambda)}$ = $0.167_{-0.025}^{+0.037}(\text{stat.}) \pm 0.012(\text{syst.})$, and $\frac{\sigma(\Omega_b^-)BR(\Omega_b^- \rightarrow J/\psi \Omega^-)}{\sigma(\Lambda_b^0)BR(\Lambda_b^0 \rightarrow J/\psi \Lambda)}$ = $0.045_{-0.012}^{+0.017}(\text{stat.}) \pm 0.004(\text{syst.})$. The acceptance and reconstruction efficiency, determined from Monte Carlo, depends on the p_T distribution at production of the Ξ_b^- and Ω_b^- . The analysis assumes that the Ξ_b^- and Ω_b^- are produced with the same p_T distribution as the Λ_b^0 . The uncertainty on the efficiencies contains contributions due to $f_{\Lambda_b^0}$, to the Monte Carlo samples size, to the simulation of the tracking system, to the Ξ^- and Ω^- branching fractions, to the uncertainty on the Λ_b^0 yield.

D0 performed the first observation of the Ξ_b^- in 1.3 fb^{-1} of data [13] and measured the mass to be $5774 \pm 11(\text{stat.}) \pm 15(\text{syst.})$ MeV/c². D0 observed also a signal of 17.8 ± 4.9 events of Ω_b^- with a significance of 5.4σ is the same decay mode as CDF. The measured Ω_b^- mass is $6.165 \pm 10(\text{stat.}) \pm 13(\text{syst.})$ shows a discrepancy of $\approx 6\sigma$ from CDF. A new analysis which uses five times more statistics is currently in progress at D0 to understand the origin of this discrepancy.

3. Measurement of the resonance properties of the Σ_b and Σ_b^* baryons

The Σ_b and Σ_b^* states have been observed at CDF as resonances in the $\Lambda_b^0 \pi^\pm$ mass distributions, where $\Lambda_b^0 \rightarrow \Lambda_c^+ \pi^-$ and $\Lambda_c^+ \rightarrow p K^- \pi^+$, using 1.1 fb^{-1} of data [14]. The $\Lambda_b^0 \pi$ states are interpreted as the lowest-lying charged Σ_b baryons and are labeled $\Sigma_b^{(*)}$. CDF has recently performed an update of this analysis using 6 fb^{-1} of data. In reconstructing the decays $\Lambda_b^0 \rightarrow \Lambda_c^+ \pi^-$ and $\Lambda_c^+ \rightarrow p K^- \pi^+$, the proton from the Λ_c^+ decay and the π^- from the Λ_b^0 decay must have $p_T > 0.5$ GeV/c. Λ_c^+ combinatorial background is also suppressed by requiring $p_T(p) > p_T(\pi^+)$. The Λ_c^+ daughter tracks are 3-D constrained to originate from a single point and the Λ_c^+ candidate is constrained to the

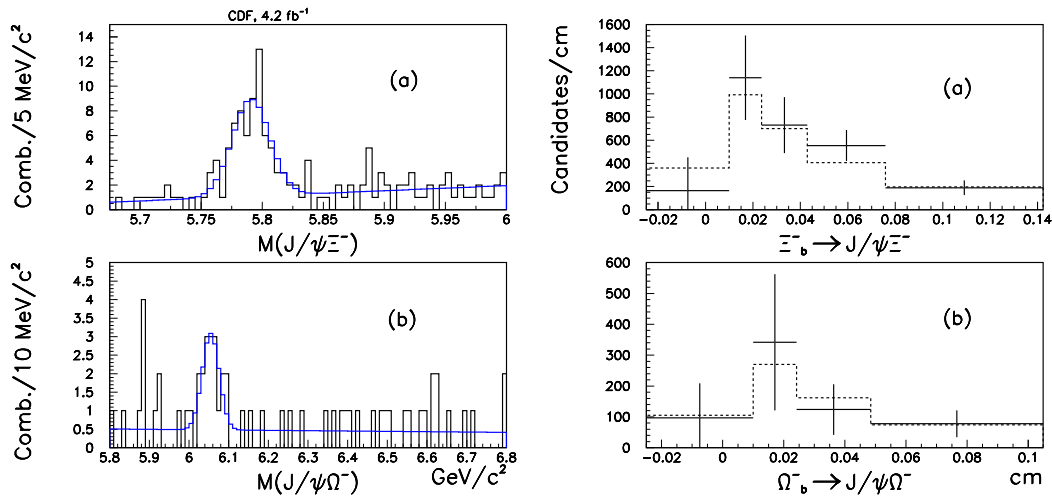


Figure 1: (Left plot) The invariant mass distributions of (a) $J/\psi \Xi^-$ and (b) $J/\psi \Omega^-$ combinations for candidates with $ct > 100 \mu\text{m}$ reconstructed at CDF. The projections of the unbinned mass fit are indicated by the blue line; (Right plot) The solid histograms represent the number of (a) $\Xi_b^- \rightarrow J/\psi \Xi^-$ and (b) $\Omega_b^- \rightarrow J/\psi \Omega^-$ candidates found in each ct bin. The dashed histogram is the fit value. (Right plot) Λ_b^0 lifetime fit performed on the data.

known Λ_c^+ mass, and the Λ_c^+ momentum is extrapolated to intersect the π^- momentum vector to form the Λ_b^0 vertex. The Λ_c^+ and Λ_b^0 must have p_T above 4.5 GeV/c and 6.0 GeV/c respectively. It is also requested $ct(\Lambda_b^0) > 200 \mu\text{m}$ and the significance $ct(\Lambda_b^0)/\sigma_{ct} > 12$, and the impact parameter of the Λ_b^0 candidate $|d_0(\Lambda_b^0)| < 80 \mu\text{m}$. The reconstruction of $\Sigma_b^{(*)}$ proceeds by combining Λ_b^0 candidates in the Λ_b^0 signal region with all remaining high quality tracks, with the pion mass hypothesis used when computing the invariant mass of the $\Sigma_b^{(*)}$ candidate. Narrow resonances are searched in the mass difference distribution of $Q = m(\Lambda_b^0 \pi) - m(\Lambda_b^0) - m_\pi$. Selection cuts are optimised to maximise the sensitivity of the search. Figure 2 reports the Q distributions reconstructed in data. The main source of background is the combination of prompt Λ_b^0 baryons, or B mesons reconstructed as Λ_b^0 baryons, with extra tracks produced in the hadronization of the b quark. An unbinned maximum likelihood fit determines the mass of the $\Sigma_b^+ = 5811.2^{+0.9}_{-0.8}(\text{stat.}) \pm 1.7(\text{syst.})$ (≈ 470 signal events), the mass of the $\Sigma_b^- = 5815.5^{+0.6}_{-0.5}(\text{stat.}) \pm 1.7(\text{syst.})$ (≈ 330 signal events), the mass of the $\Sigma_b^{*+} = 5832.0 \pm 0.7(\text{stat.}) \pm 1.8(\text{syst.})$ (≈ 780 signal events), and the mass of the $\Sigma_b^{*-} = 5835.0 \pm 0.6(\text{stat.}) \pm 1.8(\text{syst.})$ (≈ 520 signal events). The systematic errors are due to the uncertainty on the fit procedure, on the uncertainties on the momentum scale and on the assumptions made in the fitter, which include the fixed parameters describing the detector resolution and the model describing the background. A more accurate description of this analysis can be found in [15].

4. Charm baryon spectroscopy

CDF has performed an analysis of the excited charm baryons ($\Lambda_c^+(2595)$, $\Lambda_c^+(2625)$, $\Sigma_c^{0,++}(2455)$ and $\Sigma_c^{0,++}(2520)$) reconstructed in the strong decays to the Λ_c^+ ground state ($\Lambda_c^{*+} \rightarrow \Lambda_c^+ \pi^+ \pi^-$ and

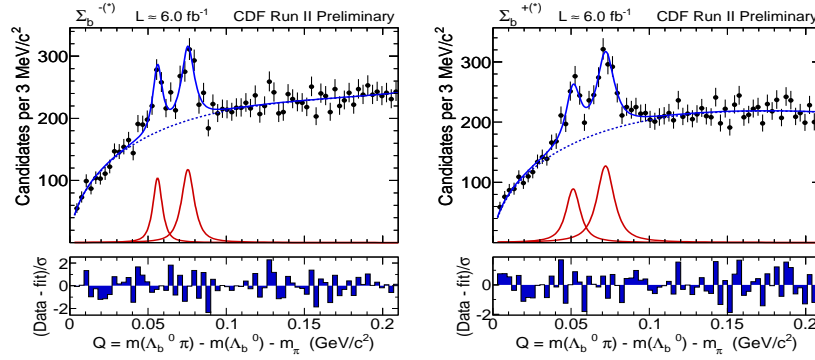


Figure 2: (Left plot) $\Sigma_b^{(*)-}$ fit to the $\Lambda_b^0\pi^-$ subsample; (Right plot) $\Sigma_b^{(*)+}$ fit to the $\Lambda_b^0\pi^+$ subsample.

$\Sigma_c^{0,++} \rightarrow \Lambda_c^+ \pi^- \pi^+$). The analysis performs a measurement of the mass differences of these resonances to the Λ_c^+ mass and of the corresponding decay widths. The $\Lambda_c^+(2595)$ mass shape is affected by kinematical threshold effects in the resonant subdecay $\Lambda_c^+(2595) \rightarrow \Sigma_c(2455)\pi$ which lead to a mass which is approximately $3 \text{ MeV}/c^2$ lower than the previously measured values. This analysis uses the highest number of signal events for all the resonances which leads to the most accurate values of the $\Lambda_c^+(2595)$ and $\Lambda_c^+(2625)$ properties[16].

5. Observation of the resonant structure of the $\Lambda_b^0 \rightarrow \Lambda_c^+ \pi^- \pi^+ \pi^-$ decay mode

CDF reconstructed a signal of 848 ± 93 $\Lambda_b^0 \rightarrow \Lambda_c^+ \pi^- \pi^+ \pi^-$ candidates with $\Lambda_c^+ \rightarrow pK^- \pi^+$ in 2.4 fb^{-1} of data (Figure 3). In the $\Lambda_b^0 \rightarrow \Lambda_c^+ \pi^- \pi^+ \pi^-$ sample we reconstructed the resonant decay modes: $\Lambda_b^0 \rightarrow \Lambda_c(2595)^+ \pi^-$ (46.6 ± 9.7 candidates), $\Lambda_b^0 \rightarrow \Lambda_c(2625)^+ \pi^-$ (114 ± 13 candidates), $\Lambda_b^0 \rightarrow \Sigma_c(2455)^{++} \pi^- \pi^-$ (81 ± 15 candidates), and $\Lambda_b^0 \rightarrow \Sigma_c(2455)^0 \pi^+ \pi^-$ (41.5 ± 9.3 candidates) (Figure 3). We measured the relative branching fractions of the resonant Λ_b^0 decay modes (Table 1), by using the signal yields estimated by performing fits of the mass distributions (Figure 3) and relative efficiency factors estimated with Monte Carlo. The main sources of systematic errors derive from the uncertainties on fits of the data and from the uncertainties on relative efficiencies estimated with the Monte Carlo simulation. The main uncertainties on the fits of the data derive from the uncertainties of the background models and from the resolution model used in the model of the resonant signals, and from the uncertainty on the contributions of the Cabibbo suppressed decay modes. The main uncertainties due to the relative efficiencies derive from the uncertainties on the Λ_c^+ , $\Lambda_c(2595)^+$, and $\Lambda_c(2625)^+$ resonant structure, from the average of the relative efficiency for the $\Lambda_b^0 \rightarrow \Lambda_c^+ \rho^0 \pi^-$ and $\Lambda_b^0 \rightarrow \Lambda_c^+ \pi^- \pi^+ \pi^-$ decay modes, which are not separated in this analysis, from the unknown Λ_b^0 and Λ_c^+ polarisations, from the uncertainty on the Λ_b^0 production transverse momentum distribution, and from the uncertainty on the Λ_b^0 and Λ_c^+ lifetimes. More details about this analysis can be found in [17].

6. *b* hadron lifetime measurement in the $J/\psi/\pi$ decay modes

CDF has performed a new *b* hadron lifetime measurement using the decay modes $B^0 \rightarrow J/\psi K^{*0}$, $B^0 \rightarrow J/\psi K_s^0$, $B^+ \rightarrow J/\psi K^+$, and $\Lambda_b^0 \rightarrow J/\psi \Lambda$ reconstructed in 4.3 fb^{-1} of data col-

$\frac{BR(\Lambda_b^0 \rightarrow \Lambda_c(2595)^+ \pi^- \rightarrow \Lambda_c^+ \pi^- \pi^+ \pi^-)}{BR(\Lambda_b^0 \rightarrow \Lambda_c^+ \pi^- \pi^+ \pi^- (all))}$	$(2.5 \pm 0.6(stat) \pm 0.5(syst)) \cdot 10^{-2}$
$\frac{BR(\Lambda_b^0 \rightarrow \Lambda_c(2625)^+ \pi^- \rightarrow \Lambda_c^+ \pi^- \pi^+ \pi^-)}{BR(\Lambda_b^0 \rightarrow \Lambda_c^+ \pi^- \pi^+ \pi^- (all))}$	$(6.2 \pm 1.0(stat)_{-0.9}^{+1.0}(syst)) \cdot 10^{-2}$
$\frac{BR(\Lambda_b^0 \rightarrow \Sigma_c(2455)^{++} \pi^- \pi^- \rightarrow \Lambda_c^+ \pi^- \pi^+ \pi^-)}{BR(\Lambda_b^0 \rightarrow \Lambda_c^+ \pi^- \pi^+ \pi^- (all))}$	$(5.2 \pm 1.1(stat) \pm 0.8(syst)) \cdot 10^{-2}$
$\frac{BR(\Lambda_b^0 \rightarrow \Sigma_c(2455)^0 \pi^+ \pi^- \rightarrow \Lambda_c^+ \pi^- \pi^+ \pi^-)}{BR(\Lambda_b^0 \rightarrow \Lambda_c^+ \pi^- \pi^+ \pi^- (all))}$	$(8.9 \pm 2.1(stat)_{-1.0}^{+1.2}(syst)) \cdot 10^{-2}$
$\frac{BR(\Lambda_b^0 \rightarrow \Lambda_c^+ \rho^0 \pi^- + \Lambda_c^+ 3\pi (other) \rightarrow \Lambda_c^+ \pi^- \pi^+ \pi^-)}{BR(\Lambda_b^0 \rightarrow \Lambda_c^+ \pi^- \pi^+ \pi^- (all))}$	$(77.3 \pm 3.1(stat)_{-3.3}^{+3.0}(syst)) \cdot 10^{-2}$

Table 1: Measured relative Branching Fractions of the resonant $\Lambda_b^0 \rightarrow \Lambda_c^+ \pi^- \pi^+ \pi^-$ decay modes.

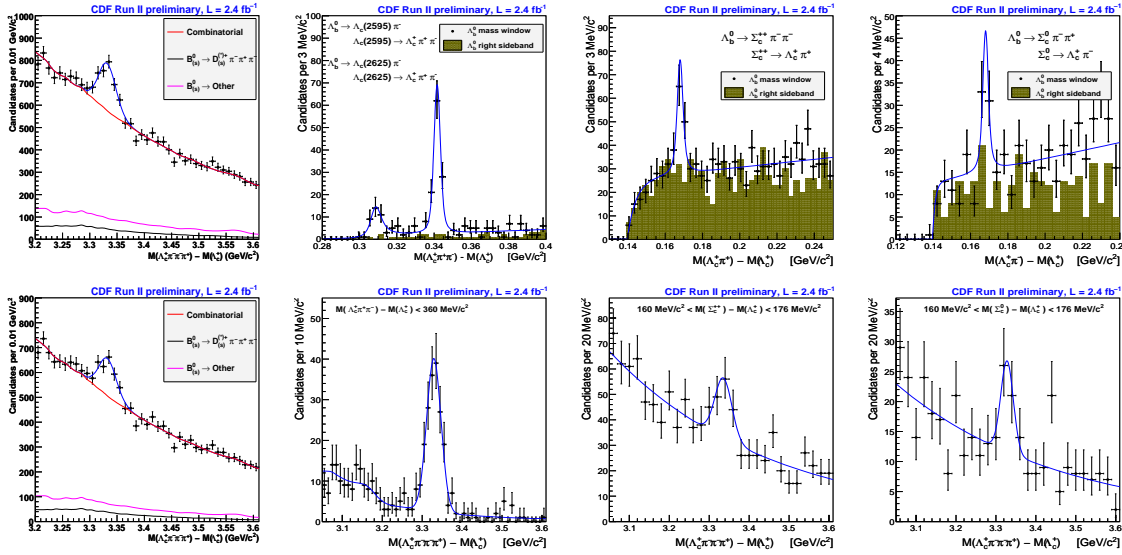


Figure 3: (Top row, first from left) $\Lambda_b^0 \rightarrow \Lambda_c^+ \pi^- \pi^+ \pi^-$ candidates mass distribution; (Top row, second from left) $\Lambda_b^0 \rightarrow \Lambda_c(2595)^+ \pi^-$ and $\Lambda_b^0 \rightarrow \Lambda_c(2625)^+ \pi^-$ candidates in a $\pm 3\sigma$ Λ_b^0 mass window ($\sigma = 16$ MeV/c^2); (Top row, third from left) $\Lambda_b^0 \rightarrow \Sigma_c(2455)^{++} \pi^- \pi^-$ candidates in a $\pm 3\sigma$ Λ_b^0 mass window; (Top row, fourth from left) $\Lambda_b^0 \rightarrow \Sigma_c(2455)^0 \pi^+ \pi^-$ candidates in a $\pm 3\sigma$ Λ_b^0 mass window; (Bottom row, first from left) $\Lambda_b^0 \rightarrow \Lambda_c^+ \pi^- \pi^+ \pi^-$ candidates mass distribution with a veto on the charm baryon resonant decay modes; (Bottom row, second from left) $\Lambda_b^0 \rightarrow \Lambda_c^+ \pi^- \pi^+ \pi^-$ candidates mass distribution in the $\Lambda_c(2595)^+$ and $\Lambda_c(2625)^+$ mass window; (Bottom row, third from left) $\Lambda_b^0 \rightarrow \Lambda_c^+ \pi^- \pi^+ \pi^-$ candidates mass distribution in the $\Sigma_c(2455)^{++}$ mass window; (Bottom row, fourth from left) $\Lambda_b^0 \rightarrow \Lambda_c^+ \pi^- \pi^+ \pi^-$ candidates mass distribution in the $\Sigma_c(2455)^0$ mass window.

lected by the dimuon trigger, which has no biasing effect on the observed proper time distribution. Signal samples of $\approx 45,000$ B^+ , $\approx 29,000$ B^0 , and $\approx 1,700$ Λ_b^0 are reconstructed. The analysis consists of a maximum likelihood fit that uses information from mass, proper decay time and proper decay time error to extract the lifetime of the hadrons. The use of similar final states and a unified analysis strategy allow partial cancellation of certain systematic uncertainties in the lifetime ratios. The measured lifetimes are the currently most precise determination of the B^+ , B^0 and Λ_b^0 lifetime. The measured values are $c\tau(B^+) = 491.4 \pm 2.6(\text{stat.}) \pm 2.6(\text{syst.}) \mu\text{m}$, $c\tau(B^0) = 451.7 \pm 3.0(\text{stat.}) \pm 2.5(\text{syst.}) \mu\text{m}$, and $c\tau(\Lambda_b^0) = 460.8 \pm 13.4(\text{stat.}) \pm 4.1(\text{syst.}) \mu\text{m}$. [18]

7. Conclusions

In this paper we reviewed the most recent results in the field of B baryons at CDF and D0. These include the observation of the Ω_b^- , Ξ_b^- , Σ_b and Σ_b^* , and the reconstruction of the new $\Lambda_b^0 \rightarrow \Lambda_c^+ \pi^- \pi^+ \pi^-$ decay mode, and the new measurement of b hadron lifetimes in the J/ψ modes.

References

- [1] D. Acosta et al., the CDF Collaboration, Phys. Rev. D 75, 012010 (2007); T. Aaltonen et al., the CDF Collaboration, Phys. Rev. D 79, 092003 (2009).
- [2] T. Aaltonen et al., the CDF Collaboration, Phys. Rev. D 79, 092003 (2009).
- [3] A. Sill et al., Nucl. Instrum. Meth. A530:1 (2004).
- [4] T. Affolder et al., Nucl. Instrum. Meth. A526:249 (2004).
- [5] D. Acosta et al., Nucl. Instrum. Meth. A518:605 (2004).
- [6] L. Balka et al., Nucl. Instrum. Meth. A267:272 (1988).
- [7] G. Ascoli et al., Nucl. Instrum. Meth. A268:33 (1988).
- [8] E. J. Thomson et al., IEEE Trans. on Nucl. Sc. vol. 49, n. 3 (2002).
- [9] W. Ashmanskas *et al.*, Nucl. Instrum. Meth. A518: 532, (2004)
- [10] V. M. Abazov *et al.*, Instrum. Meth. A565: 463, (2006)
- [11] T. Aaltonen *et al.*, Phys. Rev. D80, 072003 (2009).
- [12] V. M. Abazov *et al.*, Phys. Rev. Lett. 101, 232002 (2008).
- [13] V. M. Abazov *et al.*, Phys. Rev. Lett. 99, 052001 (2007).
- [14] T. Aaltonen *et al.*, Phys. Rev. Lett. 9, 202001 (2007).
- [15] The CDF B Group Public web page,
http://www-cdf.fnal.gov/physics/new/bottom/100721.blessed-Sigmab_6fb/
- [16] The CDF B Group Public web page,
http://www-cdf.fnal.gov/physics/new/bottom/100701.blessed-Charm_Baryons/
- [17] The CDF B Group Public web page,
<http://www-cdf.fnal.gov/physics/new/bottom/091029.blessed-Lb2Lc3pi-structure/>
- [18] The CDF B Group Public web page,
<http://www-cdf.fnal.gov/physics/new/bottom/091217.blessed-JpsiX4.3/>